Quantification of Myocardial Blood Flow Using ^{13}N-Ammonia and PET: Comparison of Tracer Models

Yong Choi, Sung-Cheng Huang, Randall A. Hawkins, Joon Young Kim, Byung-Tae Kim, Carl K. Hoh, Kewei Chen, Michael E. Phelps and Heinrich R. Schelbert

Department of Nuclear Medicine, Sungkyunkwan University School of Medicine, Samsung Medical Center, Seoul, Korea; and Division of Nuclear Medicine and Biophysics, Department of Molecular and Medical Pharmacology, UCLA School of Medicine, Los Angeles, California

Several tracer kinetic methods have been proposed for quantification of regional myocardial blood flow (MBF) with ^{13}N-ammonia and PET. Merits and limitations specific to each approach, however, generally are not clear, because they have not been evaluated in the same experimental environment. Therefore, we compared six different commonly used methods (11 modifications) to characterize the accuracy of each approach. The methods included the two-parameter model (method 1), the modified two-parameter model (method 2), the four-parameter model (method 3), the graphical analysis (method 4), the first-pass extraction method (method 5) and the dose uptake index (DUI; method 6). **Methods:** Eleven studies in four dogs, 16 studies in eight healthy human volunteers and 14 studies in seven patients were performed using ^{13}N-ammonia and PET. MBF in dogs was varied with dipyridamole and coronary occlusions and was measured independently and simultaneously with microspheres. Volunteers and patients were studied at baseline and after dipyridamole. MBF and DUI were estimated using a time-activity curve ($Q_i[t]$) derived from dynamic images and regions of interest (ROIs) and using the six methods. DUI was defined as $Q_i(t = 2\ min) \times$ weight/dose. **Results:** MBF estimated by methods 1–5 correlated well with microsphere MBF in dogs. MBF estimates by method 1 correlated well with those by methods 2, 4 and 5 and to a lesser degree with those by method 3 in both dog and human studies. DUI correlated poorly with MBF by microspheres and by methods 1–5 in both dog and human studies. MBF estimates by method 3 showed larger dispersion (SD/mean flow) and higher sensitivity to metabolites correction in arterial blood than those by methods 1, 2, 4 and 5. **Conclusion:** MBF can be measured accurately using ^{13}N-ammonia PET and tracer kinetic methods. DUI is a poor indicator of MBF values. The results indicate that preference should be given to the two-parameter model, incorporating geometrical ROI representation (method 2) among the compartment models, and to the graphical analysis (method 4) among the noncompartmental approaches.

Key Words: myocardial blood flow; ^{13}N-ammonia; PET; tracer kinetic methods

J Nucl Med 1999; 40:1045–1055

Received Mar. 24, 1998; revision accepted Nov. 4, 1998.

For correspondence or reprints contact: Byung-Tae Kim, MD, Department of Nuclear Medicine, Samsung Medical Center, 50 Ilwon-Dong, Kangnam-Ku, Seoul, Korea 135–230.

Nitrogen-13-ammonia, a tracer of myocardial blood flow (MBF), and PET have been used widely for myocardial perfusion imaging and for quantification of MBF. ^{13}N-ammonia and PET provide high-quality images, mainly because metabolically bound ^{13}N activities allow the acquisition of high and appropriate count statistics (*1*). The accuracy of MBF estimates by ^{13}N-ammonia and PET has been validated extensively at different institutions (*2–4*) in comparison with microsphere-based measurements of MBF. The noninvasiveness and technical convenience of ^{13}N-ammonia and PET for quantification of MBF allow the use of this technique to explore important physiologic questions, such as different drug effects and pharmacologic and physical exercise effects on MBF (*5,6*). Moreover, ^{13}N-ammonia and PET have been found to be useful clinically for detecting coronary artery disease and for examining myocardial viability (*7–9*).

To quantify MBF accurately with ^{13}N-ammonia and PET, however, various factors associated with the tracer and the emission CT need to be considered. These factors include the nonlinear relationship between the first-pass extraction fraction of ^{13}N-ammonia and MBF, partial volume effects on PET images, cross-contamination between blood and the myocardial region as a result of spillover of activity and contamination of the arterial input function by ^{13}N metabolites. Several different tracer kinetic methods have been proposed to address these problems and to improve quantitative accuracy. In addition, efficient analysis approaches have been developed to reduce the complexities and to facilitate the use of quantitative flow measurements in the clinical environment. Generally, these methods can be categorized as the compartment modeling approach (*3,10,11*), graphical analysis (*12*) and the first-pass extraction method (*2,13*). The merits and limitations of each approach, however, are not generally clear. This has prompted controversies on which is the better method. Therefore, there is a need to evaluate these various approaches in a common environment with, for example, the same set of data. The purpose of this study was to compare six commonly used methods with

11 different modifications for the quantification of MBF with ^{13}N-ammonia and PET in both dog and human studies.

MATERIALS AND METHODS

Animal Studies

Eleven flow measurements, including 3 at baseline, 6 during dipyridamole-induced hyperemia and 2 coronary occlusions in 4 mongrel dogs (weight range 25–32.5 kg) were used. Animal instrumentation and experimental procedures for these dog studies have been described previously (*3*). Although the experimental data used in this investigation have been reported previously (*3,12*), the comparison of different methods for quantifying MBF is presented here for the first time. Arterial blood samples (1 mL each), drawn at 40, 80, 120 and 180 s after tracer injection in each study, were used to determine the time-dependent distribution of ^{13}N-ammonia and its metabolites in whole blood (*14*). Regional MBF also was measured independently and simultaneously with each ^{13}N-ammonia injection with radioactive carbonized polystyrene microspheres (15 μm diameter; DuPont, North Billerica, MA) using the arterial reference sampling technique (*15*).

Human Studies

Five male and 3 female volunteers (age range 19–80 y, mean age 61 ± 21 y) without evidence of cardiac disease and 7 patients with arteriographically documented coronary artery disease were studied. The study protocol had been approved by the University of California at Los Angeles Human Subject Protection Committee, and each participant gave informed consent in writing. Study participants were chosen to reflect a wide range of MBF to test the different quantification methods in both normal and abnormal myocardium. MBF was determined twice with ^{13}N-ammonia, first at rest and then during dipyridamole-induced hyperemia (0.56 mg/kg dipyridamole administered intravenously over 4 min, followed 4 min later by tracer injection).

Image Acquisition and Reconstruction

All dog and human studies were performed on a Siemens/CTI 931/08–12 tomograph (Knoxville, TN), which produces 15 contiguous transaxial image planes encompassing a 108-mm axial field of view. A 2-min rectilinear-type transmission scan with a ^{68}Ge/^{68}Ga external ring source was used to assist in centering the heart within the 15-plane axial field of view. This was followed by acquisition of a 20-min transmission scan for subsequent photon attenuation correction. ^{13}N-ammonia (550–740 MBq) diluted in 10 mL saline solution was injected as a 30-s intravenous bolus by infusion pump. The intravenous line was then flushed with 10 mL saline delivered at the same infusion rate again over a 30-s period to minimize residual activities in the injection line.

Acquisition of serial emission images began just before the ^{13}N-ammonia injection and consisted of a sequence of twelve 10-s and six 20-s frames in the dog studies and of twelve 10-s, two 30-s, one 60-s and one 900-s frames in the human studies. In the dogs, four electrocardiogram gated frames of equal time duration were acquired for 20 min immediately after the dynamic imaging sequence. Studies were repeated at 50- to 60-min intervals to allow for physical decay of ^{13}N activity from the prior study. The serially acquired 15-plane transaxial images were reconstructed using a Shepp-Logan filter with a cutoff frequency of 0.96 cycles/cm, yielding a spatial resolution of about 10 mm full width at half maximum (FWHM) in plane. The scanner's axial resolution was ~7 mm FWHM.

Image Analysis

In the dog studies, the 15 contiguous transaxial images acquired in diastole as well as those acquired serially after tracer administration were reoriented into left ventricular short-axis slices as described previously (*16*). Guided by photographs of the postmortem myocardial cross-sections, 3 midventricular short-axis images were generated to match the 3 corresponding postmortem myocardial cross-sections for each animal.

Eight sectorial myocardial time-activity curves were generated using ungated dynamic images from eight equally divided (45° for each sector) sectorial regions of interest (ROIs) defined by the two contours separated radially by three pixels (1.17 mm/pixel) and centered at the peak of myocardial circumferential activity. The myocardial contours were drawn automatically on each dynamic image frame, if the myocardial uptake was sufficiently high for defining myocardial edges. If the myocardial uptake was not high enough in early frames, the myocardial contours and sectorial ROIs drawn on later image frames were copied to the initial frames.

Sectorial recovery coefficients for a given image spatial resolution, myocardial thickness and ROI thickness were derived in each imaging plane on the basis of a myocardial activity thickness estimated by profile analysis of the activity across the myocardial wall on the diastolic gated images (*17,18*).

For the study in normal human volunteers, time-activity curves for four sectors (60°–70° arcs, assigned to the interventricular septum, the anterior, lateral and posterolateral wall) in one midventricular transaxial plane were generated. Myocardial time-activity curves for hypoperfused segments (28 segments) and normal segments (28 segments) in patients with coronary artery disease were generated by defining the sectors interactively. Three-pixel (1.56 mm/pixel) wide sectorial ROIs were drawn on images obtained about 3 min after tracer injection. Sectorial myocardial time-activity curves were generated by copying these ROIs to the serially acquired transaxial dynamic image frames. A constant recovery coefficient of 0.75 was estimated by assuming a uniform myocardial activity thickness of 1 cm.

The time-activity curves of ^{13}N activity concentrations in arterial blood, AB(t), were derived from a small elliptical ROI (about 50 mm^2) assigned to the left ventricular blood pool on the dynamic images (*19–21*). These curves were generated from two midventricular imaging planes and were averaged to reduce noise. The fraction of ^{13}N metabolites of the total ^{13}N activity in whole blood was subtracted on the basis of measurement in each dog study or, in human studies, on the basis of previously reported results (*6,17*) to obtain the true arterial tracer input function, $C_a(t)$.

Calculation of Myocardial Blood Flow: Methods

The six different methods for quantification of MBF examined in this study are summarized in Table 1. The effect of the ^{13}N metabolites in arterial blood was examined for each approach.

Compartment Modeling Approach

The kinetics of ^{13}N-ammonia in the myocardium as observed by PET have been described by several compartment models (*3,4,10,11,22*). Although each modeling approach deals differently with problems related to ^{13}N-ammonia and PET, all share a basic model configuration, as illustrated in Figure 1. Compartment 1 in this model represents the concentration of ^{13}N-ammonia in arterial blood, and compartment 2 represents a space of freely diffusible ^{13}N-ammonia, including intravascular and interstitial spaces. Compartment 3 describes the metabolically bound ^{13}N activity (mostly in the form of ^{13}N-glutamine) in the myocardium. First-order rate

TABLE 1
Different Methods for Quantification of Myocardial Blood Flow

Method	Kinetic tissue data used (min)	Partial volume correction	Metabolites correction (input function)
1Y Two-parameter model	0–2	Externally	Yes
1N Two-parameter model	0–2	Externally	No
2Y Modified two-parameter model	0–2	Internally	Yes
2N Modified two-parameter model	0–2	Internally	No
3Y Four-parameter model	0 to ~10	Internally	Yes
3N Four-parameter model	0 to ~10	Internally	No
4Y Graphical analysis	1–2	Externally	Yes
4N Graphical analysis	1–2	Externally	No
5Y First-pass extraction method	2	Externally	Yes
5N First-pass extraction method	2	Externally	No
6 Dose uptake index	2	Externally	—*

*Arterial input function is not used in method 6.

Externally = partial volume effect corrected on basis of recovery coefficient; Internally = partial volume effect corrected using geometric model during model fitting.

constants k_1 to k_4 describe the rate of tracer exchange between compartments.

Two-Parameter Model. In the two-parameter model (*3,12,22*), the rate constants k_1 (mL/min/g) and k_2 (min^{-1}) represent MBF and MBF/V, respectively, where V is the distribution volume of ^{13}N-ammonia in the free space. The rate constant k_3 (mL/min/g) represents the conversion rate of freely diffusible ^{13}N-ammonia into a metabolically bound radiotracer, and k_4 (min^{-1}) is the clearance rate constant of ^{13}N activities from the bound to the free compartment.

The number of parameters estimated by model fitting was reduced to two in this model by fixing parameters to certain values or by using the relationship between parameters. During the model fitting, the relationship between k_3 and MBF (k_1),

$$k_3 = MBF[1.65e^{(1.25/MBF)} - 1], \quad \text{Eq. 1}$$

was used to correct for the nonlinear relationship between the first-pass extraction fraction of ^{13}N-ammonia and MBF (*1*) and to reduce the number of variable parameters. Equation 1 is derived by equating the extraction fraction (E_m) from the model described in Figure 1,

$$E_m = \frac{k_3}{k_3 + MBF}, \quad \text{Eq. 2}$$

to the extraction fraction (E_d) determined previously (*1*) in dog experiments,

$$E_d = 1 - 0.607e^{(-1.25/MBF)}. \quad \text{Eq. 3}$$

The kinetic data obtained 0–2 min after ^{13}N-ammonia injection were used for the model fitting. The rate constant k_4 and the distribution volume of free ^{13}N-ammonia in the myocardium (V [mL/g]) were fixed to 0 and 0.8, respectively. No minimum and maximum bounds of the parameters were applied during model fitting.

Partial-volume-effect-related underestimation of myocardial ^{13}N activity concentrations by PET was corrected using a recovery coefficient (RC). Spillover of activity from the ventricular blood pool into the myocardial ROI and from blood activity in the myocardial vascular space was accounted for by an additional parameter (f_a) in the model:

$$C_i(t)/RC = C_t(t) + f_a \times AB(t), \quad \text{Eq. 4}$$

where $C_i(t)$ is the measured myocardial ^{13}N activity concentration obtained from an ROI, $C_t(t)$ is the model-predicted myocardial ^{13}N activity concentration and AB(t) is ^{13}N activity in arterial blood obtained from the left ventricular blood-pool ROI. Finally, f_a represents the fraction of AB(t) measured in the myocardium ROI as a result of spillover from blood-pool activity into the myocardium ROI and the blood volume in the myocardium ROI.

Modified Two-Parameter Model. As a new approach, a modified two-parameter model, which incorporates a geometrical model of ROI representation in physical space (*23*) into the two-parameter model, also was examined in this study. The approach is identical to the original two-parameter model except for correction of partial volume and spillover effects by use of a geometrical model:

$$C_i(t) = (1 - f_b)C_t(t) + f_b \times AB(t), \quad \text{Eq. 5}$$

where f_b is the spillover of blood-pool activity into the myocardium ROI.

Four-Parameter Model. The four-parameter model also is derived from the compartment model, shown in Figure 1 (*4,10*). The representation of the compartments is the same as in the two-parameter method. The rate constant k_1 (mL/min/g) represents the processes of the delivery of ^{13}N-ammonia to the myocardium by blood flow and the extraction of the tracer across the capillary-tissue interface in a single capillary transit. The rate constants k_2 (min^{-1}) and k_3 (min^{-1}) represent the ^{13}N-ammonia washout rate and ^{13}N-glutamine formation rate constant, respectively. The rate

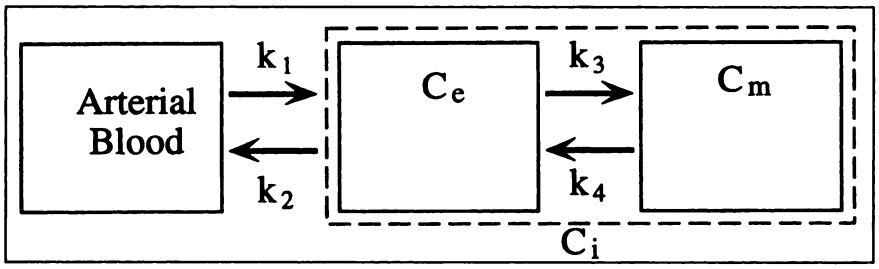

FIGURE 1. General ^{13}N-ammonia compartment model. First compartment represents concentration of ^{13}N-ammonia in arterial blood. Second and third compartments represent free ^{13}N-ammonia and metabolically bound ^{13}N-labeled metabolites, respectively. k1 to k4 are first-order rate constants.

constant k_4 was excluded in this model. MBF was obtained from the estimated k_1 using the following equation:

$$k_1 = MBF \times E = MBF(1 - e^{-PS/MBF}), \quad \text{Eq. 6}$$

where PS is the permeability-surface area product for ^{13}N-ammonia and was found to be $1.08 + 2.34 \times MBF$ in canine myocardium (*1*). The initial transcapillary first-pass extraction fraction, E, for ^{13}N-ammonia is high (>90%) over a wide range of flow. It therefore is assumed that the rate constant k_1 represents MBF with a small error (8% in 4.6 mL/min/g). Because this method has four parameters to be estimated, compared with two parameters in methods 1 and 2, kinetic data over longer time periods (about 10 min) are needed for model fitting (*4,10*). All variable estimates were constrained to positive values during the model fitting. Partial-volume and spillover effects compounded in PET-measured myocardial concentrations were corrected for using the geometrical model of ROI representation (*23*):

$$C_i(t) = (1 - f_b)C_t(t) + f_b \times AB(t). \quad \text{Eq. 7}$$

Noncompartment Modeling Approach

Graphical Analysis. To simplify the calculation of MBF by avoiding the nonlinear regression required for the compartment model approaches, a graphical analysis has been used for estimating MBF (*6,12*) with the assumption of unidirectional tracer uptake:

$$\frac{C_i(t)/RC}{C_a(t)} = K\frac{\int_0^t C_a(\tau)\,d\tau}{C_a(t)} + \frac{MBF^2V}{(MBF + k_3)^2} + f_b\frac{AB(t)}{C_a(t)}, \quad \text{Eq. 8}$$

where K, the slope of the straight portion of the plot, representing the transport of tracer from the arterial input function to the precursor pool times the fraction trapped in the bound pool, is expressed as follows:

$$K = MBF[1 - 0.607e^{(-1.25/MBF)}]. \quad \text{Eq. 9}$$

Assuming k_4 to be 0, MBF then can be measured by estimating the slope, K, of the straight portion of the graph, $C_i(t)/RC/C_a(t)$ (vertical [Y] axis) versus $\int_0^t C_a(\tau)d\tau/C_a(t)$ (horizontal [X] axis), and by using the relationship described in Equation 9. The intercept of the plot was constrained within 0.43–0.65 on the basis of previous studies (*12*).

First-Pass Extraction Method. The product of first-pass extraction fraction (E) and MBF can be estimated using the following equation, with the assumption of unidirectional tracer uptake (*2,13*):

$$MBF \times E = \frac{C_i(t)}{RC} \Big/ \left(\int_0^t C_a(\tau)\,d\tau\right). \quad \text{Eq. 10}$$

MBF is then calculated from the flow-extraction fraction relation (Eq. 3), as determined previously (*1*) in canine myocardium. Myocardial kinetic data points recorded at t = 2, 3 and 10 min postinjection were analyzed to estimate MBF by Equation 10 in this study. The results obtained using t = 2 min data, demonstrating the best correlation with those estimated by other methods, are presented.

Dose Uptake Index. To examine the feasibility of estimating an index of MBF, dose uptake index (DUI) was used:

$$DUI = \frac{C_i(t)}{RC} \Big/ \left(\frac{Dose(mCi)}{Weight(kg)}\right). \quad \text{Eq. 11}$$

Myocardial kinetic data points recorded at t = 2, 3 and 10 min postinjection were analyzed to estimate DUI by Equation 11. Again, the results obtained using t = 2 min data, which correlated best with those estimated by other methods, are presented.

Statistical Analysis

Statistical significance of correlation coefficients in a linear regression was examined using a 2-tailed Z test. Linear regression lines for different methods were compared using the F test for determining statistically significant differences between slopes and intercepts. The difference of the slope of a linear regression from unity was examined with a 95% confidence interval. Pairwise comparisons were performed using paired *t* tests. The Bonferroni correction was applied when indicated. Results were considered significant at $P < 0.05$.

RESULTS

Dog Studies

Figure 2 compares for 11 dog studies the average MBF values estimated by the six different methods with the corresponding average MBF values derived simultaneously by the microsphere arterial reference technique. Mean MBF values and SDs for each study were obtained by averaging the values for the 24 anatomic segments in each study (8 segments × 3 planes), excluding experimentally hypoperfused segments. The error bars represent 1 SD and are given for MBF values determined by microspheres and by six different methods. The correlation coefficient of 0.57 for comparison of values estimated by method 6 (DUI) and estimated by microspheres was insignificant, indicating that DUI is a poor index of MBF. Results of the other methods are correlated significantly ($P < 0.001$) with the microsphere measurements.

The regression slopes of methods 1Y (refer to Table 1 for method notations; two-parameter model), 2Y (modified two-parameter model), 2N (modified two-parameter model without metabolites correction) and 4Y (graphical analysis) did not deviate significantly from unity, whereas the slopes of the other methods (1N, 3Y, 3N, 4N, 5Y, 5N and 6) were less than unity ($P < 0.05$).

The slopes and intercepts of the linear regressions presented in Figure 2 did not differ significantly from each other, with the exception of values obtained by methods 3N (four-parameter model without metabolites correction) and 6 (DUI), which were significantly ($P < 0.05$) different from those by the other methods.

Relative dispersion of regional MBF values (SD/mean flow) in normal myocardium can be an indicator of the stability of a method, because normal MBF should be homogeneous. Relative dispersions for 24 segments, excluding ischemic segments, are listed in Table 2 for each study for the microsphere approach and for the six different methods. Regional MBF estimates by microspheres showed the lowest dispersion values (0.12). Methods 2 and 6 demonstrated low dispersions (0.15 and 0.14, respectively),

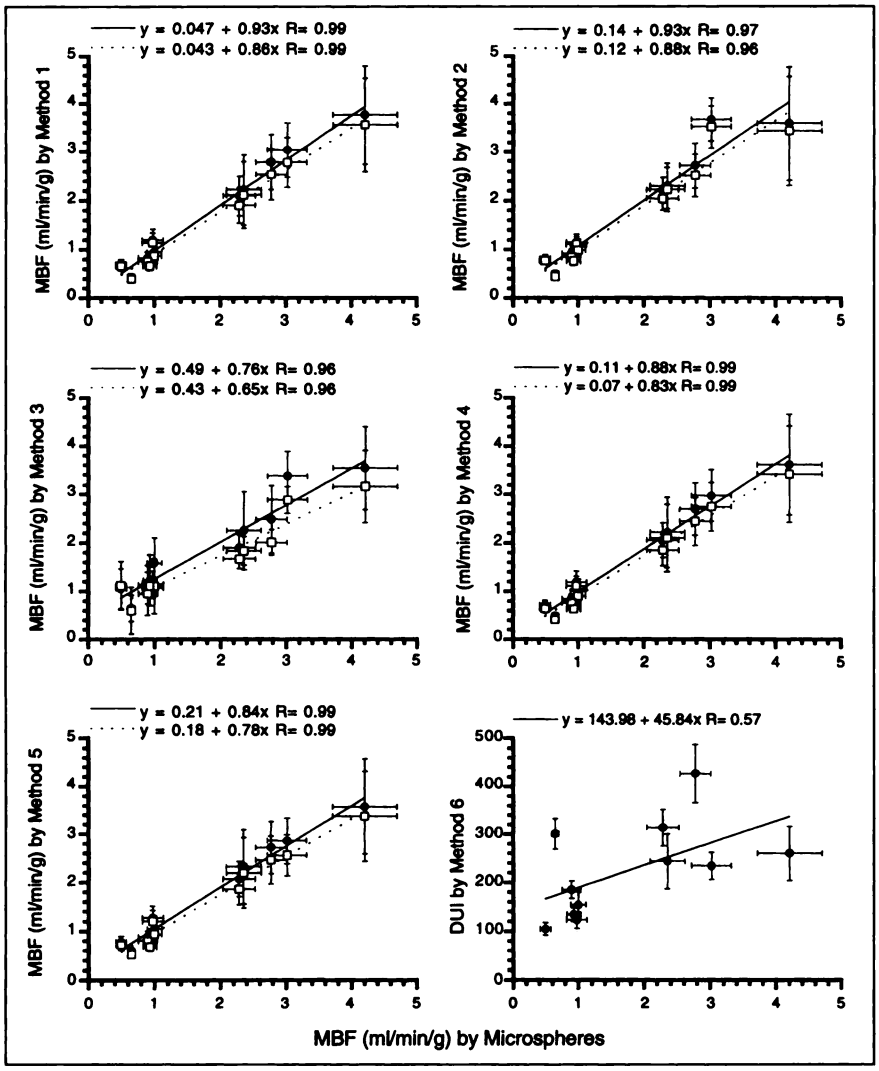

FIGURE 2. Comparison of MBF estimates by microspheres and by six methods in 11 dog studies. Solid circles = after metabolites correction; open squares = without metabolites correction; solid line = regression line to data points of solid circles; dashed line = regression line to data points of open squares.

whereas the dispersion values for methods 1, 4 and 5 (first-pass extraction method) ranged from 0.19 to 0.20. Method 3Y revealed a relative dispersion significantly higher ($P < 0.05$) than the values observed for the microsphere approach.

Table 3 lists the effect of metabolite correction in arterial blood on MBF values. Methods 1 and 2 were affected the least (6.95% and 5.69%, respectively). Correction for metabolites increased MBF values estimated by methods 4 and 5 by about 8%. Method 3 demonstrated significantly ($P < 0.05$) higher (12.7%) sensitivity to the correction for metabolites than method 2.

Figure 3 shows the comparison of MBF values estimated by method 1 with those estimated by methods 2, 4, 5 and 6. MBF estimated by methods 2, 4 and 5 correlated well with MBF values estimated by method 1. Figure 3 reveals that DUI does not adequately represent MBF and shows individual animal-dependent slopes.

Figure 4 shows the comparison of MBF values estimated by method 3 with those estimated by methods 1 and 2. The results by the compartment modeling approaches are found to correlate reasonably well, although the data scatter about the linear regression line is high.

Human Studies

Table 4 summarizes the values for MBF or DUI at rest and at stress and MBF reserve (ratio of hyperemic to rest MBF) by the six different methods in the eight healthy volunteers. Method 2 (modified two-parameter model) revealed the highest MBF reserve, 3.3. Methods 5 (first-pass extraction method) and 6 (DUI) revealed significantly ($P < 0.01$) lower MBF reserve estimates than those by method 2. Methods 1 (two-parameter model), 3 (four-parameter model) and 4 (graphical analysis) provided similar values of MBF reserve estimates, 2.9 or 3.0. Figure 5 also shows the comparisons of MBF reserve estimates in the eight healthy volunteers and seven patients. The values for relative dispersions of MBF or DUI estimates in the 16 healthy human studies are summarized in Table 5. The values were comparable for all methods except for method 3, which revealed a significantly higher relative dispersion value.

Figure 6 compares MBF values estimated by method 1 with

TABLE 2
Relative Dispersion of Different Methods: Dog Studies

Subject no.	Method											
	Microspheres	1Y	1N	2Y	2N	3Y*	3N	4Y	4N	5Y	5N	6
1	0.16	0.18	0.18	0.14	0.14	0.23	0.21	0.19	0.18	0.18	0.18	0.13
2	0.11	0.32	0.32	0.20	0.20	0.36	0.16	0.33	0.33	0.33	0.33	0.23
3	0.16	0.14	0.13	0.10	0.10	0.39	0.45	0.14	0.14	0.16	0.15	0.12
4	0.10	0.18	0.19	0.12	0.13	0.15	0.10	0.18	0.18	0.17	0.17	0.12
5	0.11	0.22	0.22	0.14	0.14	0.33	0.51	0.25	0.25	0.25	0.25	0.18
6	0.16	0.16	0.15	0.10	0.10	0.35	0.47	0.11	0.11	0.13	0.13	0.10
7	0.11	0.19	0.19	0.12	0.12	0.14	0.12	0.17	0.18	0.17	0.17	0.12
8	0.09	0.20	0.21	0.17	0.17	0.28	0.13	0.20	0.20	0.20	0.20	0.14
9	0.08	0.13	0.13	0.15	0.14	0.42	0.81	0.14	0.15	0.13	0.12	0.11
10	0.11	0.15	0.15	0.12	0.12	0.43	0.36	0.14	0.13	0.13	0.13	0.11
11	0.12	0.27	0.27	0.33	0.33	0.24	0.24	0.29	0.29	0.28	0.28	0.22
Average	0.12	0.20	0.20	0.15	0.15	0.30	0.32	0.20	0.19	0.19	0.19	0.14
SD	0.03	0.06	0.06	0.07	0.07	0.10	0.22	0.07	0.07	0.07	0.07	0.05

*Values are significantly ($P < 0.05$) higher than values for microsphere method on basis of 2-tailed paired t test after Bonferroni correction.
Values represent relative dispersion (SD/mean flow) for 24 segments, excluding ischemic segments, in 11 dog studies.

those estimated by methods 2–6 for eight healthy volunteers (16 studies, 64 sectors) and for seven patients (14 studies, 56 sectors). MBF values estimated by method 1 correlated well with MBF values estimated by methods 4 ($r = 0.97$) and 5 ($r = 0.93$) and to lesser degree with method 2 ($r = 0.85$). Correlation with method 3 was relatively poor, mainly as the result of several outliers. DUI did not adequately reflect flow values, especially in high MBF regions.

Figure 7 shows parametric images of MBF obtained by methods 4 and 5. The images are generated by applying Equations 8 or 10 to each image pixel (*10*). The parametric images generated by method 4 show superior quality to those by method 5, because method 4 uses seven kinetic data points, whereas method 5 uses one data point. Myocardial tissue to blood-pool contrast is also higher in the parametric image generated by method 4.

TABLE 3
Effect of Metabolite Correction on Myocardial Blood Flow

Subject no.	Method				
	1	2	3	4	5
1	4.70	3.75	6.47	6.83	5.71
2	4.74	3.26	18.75	5.28	5.46
3	5.59	4.83	−5.89	9.55	7.94
4	8.49	4.27	14.67	7.69	10.49
5	7.96	6.80	30.12	10.11	10.09
6	8.25	7.77	16.50	9.87	9.44
7	9.35	7.76	12.24	9.75	10.09
8	8.95	7.36	19.07	9.50	9.52
9	10.71	10.42	7.57	15.02	11.75
10	2.22	1.94	9.58	2.77	2.87
11	5.47	4.47	10.65	5.50	5.68
Average	6.95	5.69	12.70*	8.35	8.09
SD	2.56	2.51	9.08	3.26	2.77

*Significantly ($P < 0.05$) high compared with values estimated by method 2.
Values are percent ratios (e.g., [1Y − 1N]/1Y × 100) of myocardial blood flow values estimated with metabolites correction to values estimated without metabolites correction in dog studies.

DISCUSSION

Different approaches for estimating MBF with ^{13}N-ammonia and PET were compared in this study. The method of choice should be determined by quantitative accuracy and methodological simplicity. The optimal method should provide the most robust and accurate MBF values and require the least mathematical, computational and methodological complexity.

Comparison to Microsphere-Determined Myocardial Blood Flow Values

The accuracy of the various noninvasive approaches was assessed in dog studies by comparison of MBF values determined by the microsphere-arterial reference sampling technique, which was the gold standard. In this comparison, the DUI was a poor indicator of MBF and failed to correlate with microsphere-determined MBF values. The comparison also indicated that the MBF values estimated by methods 1Y (two-parameter model with metabolites correction), 2Y (modified two-parameter model with metabolites correction), 2N (modified two-parameter model without metabolites correction) and 5Y (graphical analysis with metabolites correction) were not different statistically from the MBF values determined by microspheres (Fig. 2). The MBF values estimated by method 5 (first-pass extraction method) produced linear regression results slightly less than the line of identity. Method 3 (four-parameter model) led to a

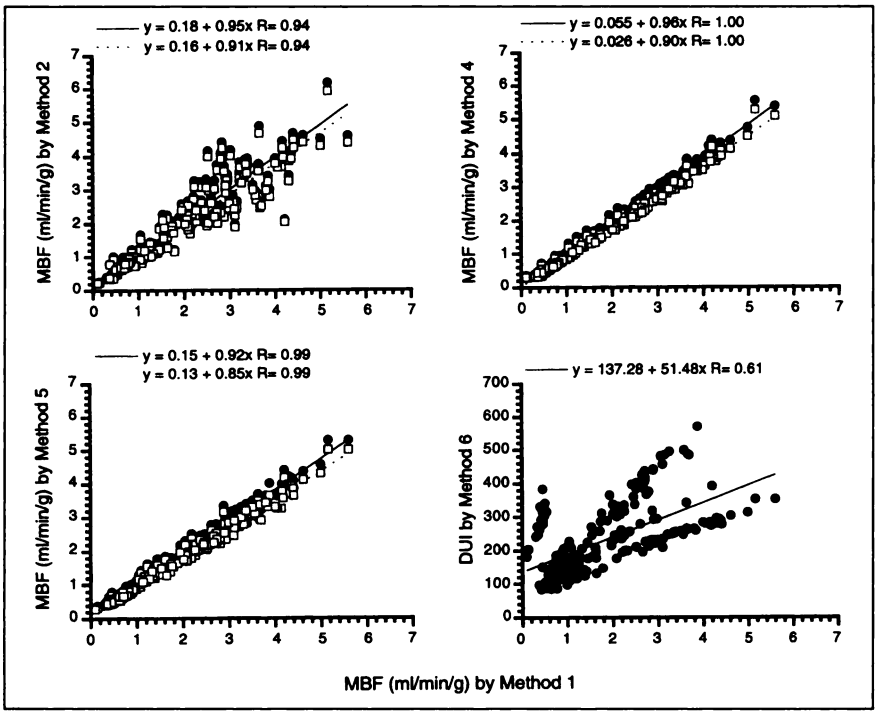

FIGURE 3. Comparison of regional MBF (264 myocardial segments) estimated by method 1 and by methods 2, 4, 5 and 6 in 11 dog studies. Solid circles = after metabolites correction; open squares = without metabolites correction; solid line = regression line to data points of solid circles; dashed line = regression line to data points of open squares.

consistent ~25% underestimation of blood flow. This underestimation may be attributed, at least in part, to the specific ROI location used in this study (*23*). To satisfy the assumptions of method 3, ROIs should be drawn at more endocardial locations, whereas in this study the ROI was drawn around the peak myocardial activity.

Relative Dispersion for Each Study

Blood flow in normal myocardium can be assumed to be fairly homogeneous, especially when relatively large tissue samples are being investigated. Thus, the coefficient of variation of regional MBFs, also referred to as "relative dispersion," should be relatively small. Besides spatial and temporal heterogeneities, method-related heterogeneities may account largely for differences in the relative dispersion between techniques. Assuming spatial and temporal relative dispersions to be constant, differences in relative dispersions between measurement approaches therefore must reflect method-related error estimates. The high dispersion values for method 3 (Tables 2 and 5, Figs. 4 and 6) indicate a high sensitivity of the method to data noise. This can be explained by the fact that method 3 has four independent parameters to estimate during the model fitting, whereas methods 1 and 2 have only two parameters.

Myocardial Blood Flow Reserve in Healthy Humans

Because of the absence of a gold standard of flow measurements by microspheres in human studies, it remains uncertain which of the various approaches will yield MBF values that approach most closely true MBF values. This limits the intermethod comparison. However, even if a specific method is associated with a systematic over- or underestimation of flows, such error should be canceled out when the myocardial flow reserve as the ratio of hyperemic to rest blood flow is estimated, and MBF reserves should be identical if all approaches are equally valid or accurate. Although the true MBF reserve again remains undetermined, the method providing the highest values of MBF reserve can be considered as the most sensitive method to estimate the parameter. Method 2 produced significantly ($P < 0.05$) higher MBF reserve than

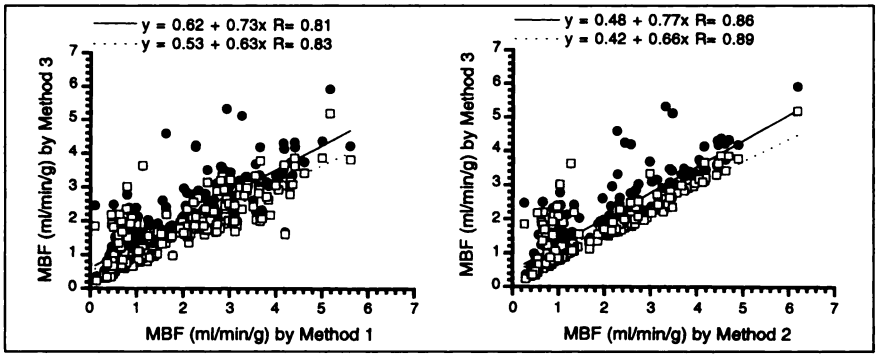

FIGURE 4. Comparison of regional MBF (264 myocardial segments) estimated by method 3 (four-parameter model) and by methods 1 (two-parameter model) and 2 (modified two-parameter model) in 11 dog studies. Solid circles = after metabolites correction; open squares = without metabolites correction; solid line = regression line to data points of solid circles; dashed line = regression line to data points of open squares.

TABLE 4
Myocardial Blood Flow or Dose Uptake Index and Myocardial Blood Flow Reserve in Healthy Humans

	Method					
	1	2	3	4	5	6
Rest	0.68 ± 0.14	0.85 ± 0.21	1.08 ± 0.36	0.65 ± 0.13	0.84 ± 0.22	124.75 ± 35.49
Stress	1.87 ± 0.45	2.63 ± 0.48	2.84 ± 1.10	1.83 ± 0.49	2.02 ± 0.44	220.08 ± 33.97
Myocardial blood flow reserve	2.86 ± 0.94	3.27 ± 1.12	2.86 ± 1.35	2.89 ± 0.94	2.48 ± 0.58*	1.87 ± 0.56*

*Significantly ($P < 0.01$) lower than values estimated by method 2.
Values are mean ± SD in eight healthy human volunteers. Myocardial blood flow is in units of mL/min/g.

methods 5 and 6. Methods 1, 3 and 4 produced similar MBF reserve values as method 2.

Metabolites Correction in Arterial Blood Input Function

^{13}N-labeled metabolites appear in blood soon after ^{13}N-ammonia injection and increase as a function of time. The time-activity curves derived from the blood-pool ROI on dynamic images will overestimate ^{13}N-ammonia activity in arterial blood (*12*). If blood-pool time-activity curves contaminated by ^{13}N-labeled metabolites are used directly as the tracer input function for calculation of MBF, the results will be underestimated. Moreover, the magnitude of the underestimation will increase as later kinetic data points are used for model fitting, because the proportion of ^{13}N-ammonia metabolites increases with time. The method that is least affected by correction for labeled metabolites will be preferred. Method 2 proved to be the least sensitive approach to such correction, whereas method 3 proved to be

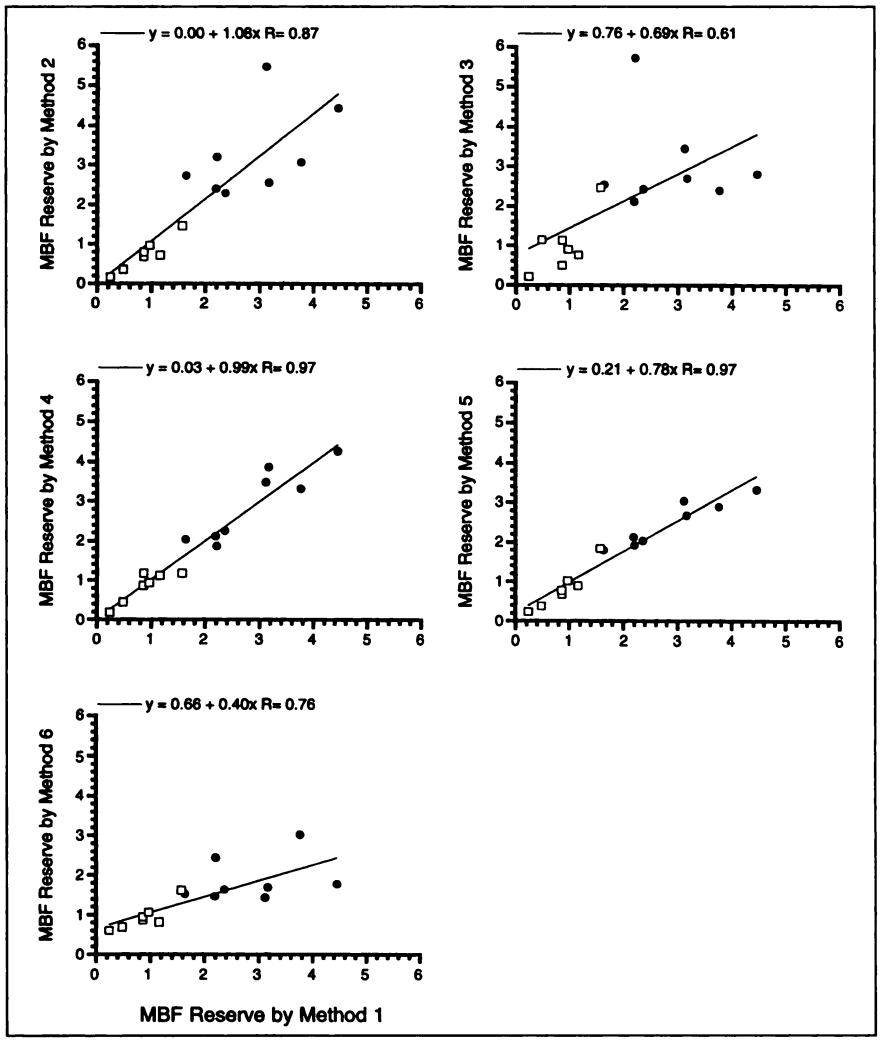

FIGURE 5. Comparison of MBF reserve values estimated by method 1 and by methods 2–6 in eight healthy individuals (solid circles) and seven patients (open squares).

TABLE 5
Relative Dispersion of Different Methods: Healthy Human Studies

Subject no.	Method 1	2	3	4	5	6
1	0.13	0.13	0.14	0.15	0.12	0.09
2	0.22	0.27	0.23	0.21	0.18	0.13
3	0.25	0.26	0.21	0.21	0.17	0.12
4	0.10	0.16	0.10	0.06	0.07	0.05
5	0.11	0.09	0.10	0.24	0.14	0.11
6	0.38	0.21	0.11	0.25	0.24	0.17
7	0.18	0.26	0.22	0.21	0.11	0.09
8	0.09	0.09	0.13	0.08	0.14	0.10
9	0.05	0.04	0.07	0.14	0.12	0.09
10	0.11	0.18	0.12	0.14	0.18	0.13
11	0.14	0.04	0.18	0.13	0.12	0.10
12	0.02	0.27	0.19	0.04	0.20	0.14
13	0.20	0.29	0.73	0.20	0.16	0.13
14	0.10	0.09	0.09	0.07	0.09	0.06
15	0.19	0.20	0.43	0.19	0.15	0.13
16	0.14	0.12	0.08	0.12	0.13	0.09
Average	0.15	0.17	0.20*	0.15	0.14	0.11
SD	0.09	0.09	0.17	0.07	0.04	0.03

*Significantly ($P < 0.05$) higher than values estimated by method 6.

Values represent relative dispersion (SD/mean flow) for four segments in 16 healthy human studies.

the most sensitive. Most likely, these method-dependent differences resulted from the different time periods of kinetic data used in the model fitting. Methods 1 and 2 fit the kinetic data of the first 2 min, whereas method 3 fit the kinetic data obtained at about 10 min.

Finite Image Resolution

Because of the finite spatial resolution of PET images, myocardial time-activity curves derived from PET images are compounded by partial-volume effect and by spillover of activity from blood pools into the myocardium (*15,16*). Input functions derived from blood-pool ROI on dynamic images also can be contaminated by spillover of activity from the myocardium to blood pools, which is more prominent at later scan times.

In methods 1, 4, 5 and 6, partial-volume effect was corrected on the basis of a recovery coefficient that was determined as a function of myocardial wall thickness, image resolution and ROI thickness. Myocardial wall thickness could be estimated from anatomic images such as echocardiogram and MRI and also from PET images, using cross-sectional profile-fitting analysis (*15,16*). Although such corrections based on measured wall thickness are likely to provide the most accurate MBF estimates, use of the same estimated recovery coefficient introduces a systemic error for all approaches that somehow cancel out in these intercomparison analysis methods.

Spillover of activity from blood pools to the myocardium was considered in method 1 as an additional parameter and in method 4 as an intercept (Eq. 8). In methods 5 and 6, the spillover of activity from blood pools to the myocardium was not corrected, thus these methods can significantly overestimate MBF values in low-flow regions or conditions. The overestimation in low-flow conditions probably is the main reason for the low MBF reserve values estimated by these two methods (Table 4, Fig. 5) and for the low ratios of normal MBF to hypoperfused MBF in patients.

In methods 2 and 3, partial volume effect and spillover activity were compensated for during the model fitting using a geometrical model of equations 5 and 7 (*23*). This approach, previously used for analyzing ^{15}O-water studies (*24*), can correct conveniently for the partial-volume effect and is shown to provide good results in this study (Fig. 2).

Simplicity of Method

Method 6 does not require the input function and is the easiest index to estimate. Methods 4 and 5 have about the same degree of simplicity in their implementation. Both methods are sufficiently computationally simple to generate parametric images of MBF by applying the methods to each image pixel. Compartment model approaches, methods 1, 2 and 3, are computationally more demanding because they require nonlinear regression for model fitting.

Method 1 versus Method 3

Methods 1 and 3 are commonly called, respectively, the two-compartment model and three-compartment model approaches. However, both methods use the same compartmental model (Fig. 1). The different names depend on whether the blood pool is considered as a separate tracer compartment. Although both methods use the same model configuration, they differ in a few aspects. In methods 1 and 2, the relationship between MBF and extraction fraction (Eq. 5) derived previously from dog studies is used. The empirically derived relationship is not validated in human studies, and the magnitude of the error caused by applying the relationship derived from dog studies to human heart, although expected to be small, remains to be determined.

In method 3, four individual parameters (k_1 [MBF], k_2, k_3, f_b) are estimated using the model fitting, whereas in methods 1 and 2, two parameters (MBF, f_b) are estimated. Because methods 1 and 2 have fewer parameters to estimate, only the first 2 min of data are used for the model fitting, whereas method 3 needs to fit more data points (about 10 min). Using shorter kinetic data will minimize certain experimental errors, such as subject motion artifact and contamination of input function by ^{13}N metabolites and by spillover of activity from the myocardium to blood pools. This also will ensure that the rate constants are more truly constant within the time interval. For example, k_1 (MBF in Fig. 1) is assumed to be a constant parameter in both models. It would be more reasonable to assume MBF is constant for the first 2 min than for 10 min, especially in pharmacologically stressed studies. In addition, because methods 1 and 2 have

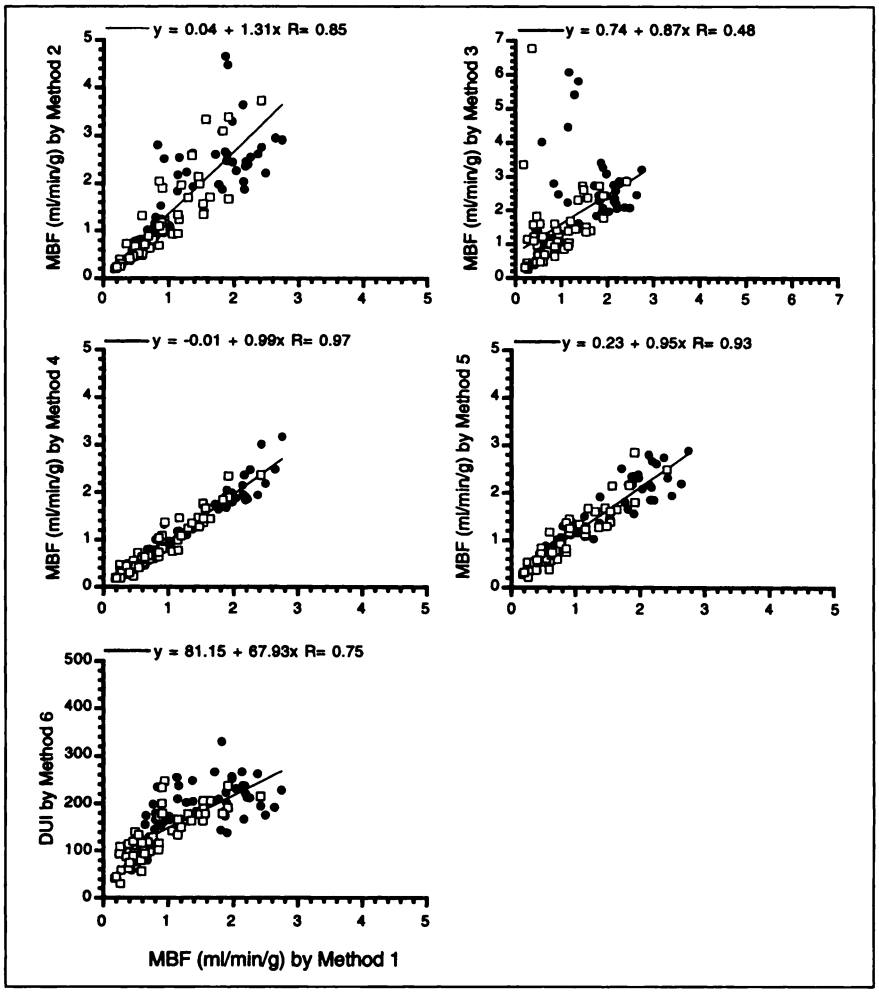

FIGURE 6. Comparison of regional MBF estimated by method 1 and by methods 2–6 in eight healthy individuals (16 studies, 64 sectors, solid circles) and seven patients (14 studies, 56 sectors, open squares).

fewer parameters to estimate, the methods provide more stable MBF values (i.e., smaller relative dispersions) than method 3, as shown in Tables 2 and 5.

Method 4 versus Method 5

MBF values estimated by method 4 showed better correlations with microsphere-determined MBF values (Fig. 2) and with MBF values determined by method 1 (Figs. 3 and 6) than the values estimated by method 5. Method 4 uses more myocardial kinetic data points than method 5. For example, method 4, using 70- to 120-s myocardial data, uses six kinetic data points, whereas method 5 uses a single time point at 2 min. In addition, it is difficult to account for the spillover of activity from blood pools to the myocardium in method 5, whereas in method 4, the spillover is considered by the intercept of the linear plot (Eq. 11). As a result, method 4 provides parametric images of MBF of a quality superior to those provided by method 5.

CONCLUSION

This study confirms the accuracy of noninvasive measurements of regional MBF with ^{13}N-ammonia, PET and tracer kinetic methods including compartmental and noncompartmental approaches. DUI is a poor indicator of MBF values. Compartment modeling approaches are physiologically well characterized but are methodologically more complicated. Noncompartmental analyses are easier to implement, but the

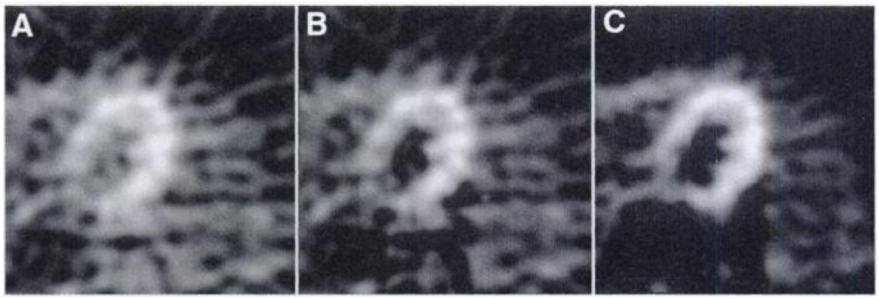

FIGURE 7. (A) ^{13}N-ammonia PET images obtained 2 min postinjection of tracer in normal subject. (B) Parametric image of MBF generated by method 5 (first-pass extraction method). (C) Parametric image of MBF generated by method 4 (graphical analysis).

limitations and assumptions of the methods should be understood before the methods are applied. The method of choice should be based on the clinical and investigative question of interest. The results presented in this study indicate that, among the compartment models, preference should be given to the two-parameter model incorporating geometrical ROI representation (method 2) and, among the noncompartmental approaches, preference should be given to graphical analysis (method 4).

ACKNOWLEDGMENTS

This study was supported in part by a grant from the 1998 Good Health R&D Project, Ministry of Health and Welfare, Republic of Korea; by Samsung grant SBRI C-97–023; by research grants HL 36232 from the National Institutes of Health, Bethesda, MD; and by U.S. Department of Energy contract DE-FC 0387-ER60615. We thank Dr. William G. Kuhle for providing valuable experimental data and for many helpful discussions regarding this work and Eileen Rosenfeld for her secretarial assistance in preparing the manuscript.

REFERENCES

1. Schelbert HR, Phelps ME, Huang SC, et al. N-13 ammonia as an indicator of myocardial blood flow. *Circulation.* 1981;6:1259–1272.
2. Bellina CR, Parodi O, Camici P, et al. Simultaneous in vitro and in vivo validation of nitrogen-13-ammonia for the assessment of regional myocardial blood flow. *J Nucl Med.* 1990;31:1335–1343.
3. Kuhle W, Porenta G, Buxton D, et al. Quantification of regional myocardial blood flow using N-13 ammonia and reoriented dynamic positron emission tomographic imaging. *Circulation.* 1992;86:1004–1017.
4. Musik O, Beanlands RSB, Hutchins GD, Mangner TJ, Nguyen N, Schwaiger M. Validation of nitrogen-13-ammonia tracer kinetic model for quantification of myocardial blood flow using PET. *J Nucl Med.* 1993;34:83–91.
5. Chan SY, Brunken RC, Czernin J, et al. Comparison of maximal myocardial blood flow during adenosine infusion with that of intravenous dipyridamole in normal men. *J Am Coll Cardiol.* 1992;20:979–985.
6. Müller P, Czernin J, Choi Y, et al. Effect of exercise supplementation during adenosine infusion on hyperemic blood flow and flow reserve. *Am Heart J.* 1994;1228:52–60.
7. Demer LL, Gould KL, Goldstein RA, et al. Assessment of coronary artery disease severity by positron emission tomography: comparison with quantitative arteriography in 193 patients. *Circulation.* 1989;79:825–835.
8. Tillisch J, Brunken RC, Marshall R, et al. Reversibility of cardiac wall motion abnormalities predicted by positron emission tomography. *N Engl J Med.* 1986;314:884–888.
9. Gewirtz H, Skopicki HA, Abraham SA, et al. Quantitative PET measurements of regional myocardial blood flow: observations in humans with ischemic heart disease. *Cardiology.* 1997;88:62–70.
10. Hutchins GD, Schwaiger M, Rosenspire KC, et al. Noninvasive quantification of regional blood flow in the human heart using N-13 ammonia and dynamic positron emission tomographic imaging. *J Am Coll Cardiol.* 1990;15:1032–1042.
11. DeGrado TR, Hanson MW, Turkington TG, et al. Estimation of myocardial blood flow for longitudinal studies with ^{13}N-labeled ammonia and positron emission tomography. *J Nucl Cardiol.* 1996;3:494–507.
12. Choi Y, Huang SC, Hawkins RA, et al. A simplified method for quantification of myocardial blood flow using N-13 ammonia and dynamic PET. *J Nucl Med.* 1993;34:488–497.
13. Shah A, Schelbert HR, Schwaiger M, et al. Measurement of regional myocardial blood flow with N-13 ammonia and positron-emission tomography in intact dogs. *J Am Coll Cardiol.* 1985;5:92–100.
14. Rosenspire KC, Schwaiger M, Mangner TJ, Hutchins GD, Sutorik A, Kuhl DE. Metabolic fate of [^{13}N]ammonia in human and canine blood. *J Nucl Med.* 1990;31:163–167.
15. Heymann M, Payne B, Hoffman J, Rudolph A. Blood flow measurements with radionuclide-labeled particles. *Prog Cardiovasc Dis.* 1977;20:55–79.
16. Kuhle W, Porenta G, Huang SC, Phelps ME, Schelbert HR. Issues in the quantitation of reoriented cardiac PET images. *J Nucl Med.* 1992;33:1235–1242.
17. Porenta G, Kuhle W, Sinha S, et al. Parameter estimation of cardiac geometry by ECG-gated PET imaging: validation using magnetic resonance imaging and echocardiography. *J Nucl Med.* 1995;36:1123–1129.
18. Gambhir SS. *Quantification of the physical factors affecting the tracer kinetic modeling of cardiac positron emission tomography data* [dissertation]. Los Angeles, CA: University of California; 1990.
19. Choi Y, Hawkins RA, Huang SC, et al. Parametric images of myocardial metabolic rate of glucose generated from dynamic cardiac PET and 2-[^{18}F]fluoro-2-deoxy-D-glucose studies. *J Nucl Med.* 1991;32:733–738.
20. Weinberg IN, Huang SC, Hoffman EJ, et al. Validation of PET-acquired input functions for cardiac studies. *J Nucl Med.* 1988;29:241–247.
21. Gambhir SS, Schwaiger M, Huang SC, et al. Simple noninvasive quantification method for measuring myocardial glucose utilization in humans employing positron emission tomography and fluorine-18-deoxyglucose. *J Nucl Med.* 1989;30:356–366.
22. Krivokapich J, Smith GT, Huang SC, et al. N-13 ammonia myocardial imaging at rest and with exercise in normal volunteers: quantification of absolute myocardial perfusion with dynamic positron emission tomography. *Circulation.* 1989;80:1328–1337.
23. Hutchins GD, Caraher JM, Raylman RR. A region of interest strategy for minimizing resolution distortions in quantitative myocardial PET studies. *J Nucl Med.* 1992;33:1243–1250.
24. Iida H, Kanno I, Takahashi A, et al. Measurement of absolute myocardial blood flow with $H_2{}^{15}O$ and dynamic positron emission tomography: strategy for quantification in relation to the partial volume effect. *Circulation.* 1988;78:104–115.